Atmos. Chem. Phys. Discuss., 13, 21159–21201, 2013
www.atmos-chem-phys-discuss.net/13/21159/2013/
doi:10.5194/acpd-13-21159-2013

Atmospheric Chemistry and Physics Discussions

The impact of satellite-adjusted NO_x emissions on simulated NO_x and O_3 discrepancies in the urban and outflow areas of the Pacific and Lower Middle US

Y. Choi

University of Houston, Department of Earth and Atmospheric Sciences, 312 Science & Research Building 1, Houston, TX 77204, USA

Received: 12 June 2013 – Accepted: 3 August 2013 – Published: 13 August 2013

Correspondence to: Y. Choi (ychoi6@uh.edu)

Published by Copernicus Publications on behalf of the European Geosciences Union.

Abstract

We analyze the simulation results from a CMAQ model and GOME-2 NO_2 retrievals over the United States for August 2009 to estimate the model-simulated biases of NO_x concentrations over six geological regions (Pacific Coast = PC, Rocky Mountains = RM, Lower Middle = LM, Upper Middle = UM, Southeast = SE, Northeast = NE). By comparing GOME-2 NO_2 columns to corresponding CMAQ NO_2 columns, we produced satellite-adjusted NO_x emission ("GOME2009") and compared baseline emission ("BASE2009") CMAQ simulations with GOME2009 CMAQ runs. We found that the latter exhibited decreases of −5.6 %, −12.3 %, −21.3 %, and −15.9 % over the PC, RM, LM, and SE regions, respectively, and increases of +2.3 % and +10.0 % over the UM and NE regions. In addition, we found that changes in NO_x emissions generally mitigate discrepancies between the surface NO_x concentrations of baseline CMAQ and those of AQS at EPA AQS stations (mean bias of +19.8 % to −13.7 % over PC, −13.8 % to −36.7 % over RM, +149.7 % to −1.8 % over LM, +22.5 % to −7.8 % over UM, +31.3 % to −7.9 % over SE, and +11.6 % to +0.7 % over NE). The relatively high simulated NO_x biases from baseline CMAQ over LM (+149.7 %) are likely the results of over-predictions of simulated NO_x emissions, which could shed light on those from global/regional Chemical Transport Models.

We also perform more detailed investigations on surface NO_x and O_3 concentrations in two urban and outflow areas, PC (e.g., Los Angeles, South Pasadena, Anaheim, La Habra and Riverside) and LM (e.g., Houston, Beaumont and Sulphur). From two case studies, we found that the GOME2009 emissions decreased surface NO_x concentrations significantly in the urban areas of PC (up to 30 ppbv) and in those of LM (up to 10 ppbv) during the daytime and that simulated NO_x concentrations from CMAQ with GOME2009 compare well to those of in-situ AQS observations. A significant reduction in NO_x concentrations resulted in a comparable increase in surface O_3 concentrations in the urban areas of PC (up to 30 ppbv) and the resulting simulated O_3 concentrations compare well with in-situ surface O_3 observations over South Pasadena, Ana-

ACPD
13, 21159–21201, 2013

heim, and Riverside. Over Houston, Beaumont, and Sulphur, large reductions in NO_x emissions from CMAQ with GOME2009 coincides with large reduced concentrations of simulated NO_x. These concentrations are similar to those of the EPA AQS NO_x observations. However, the resulting simulated increase in surface O_3 at the urban stations in Houston and Sulphur exacerbated preexisting high O_3 over-predictions of the baseline CMAQ. This study implies that simulated low O_3 biases in the urban areas of PC are likely caused by simulated high NO_x biases, but high O_3 biases in the urban areas of LM cannot be explained by simulated high NO_x biases over the region. This study also suggests that both in-situ surface NO_x and O_3 observations should be used simultaneously to resolve issues pertaining to simulated high/low O_3 bias and that remote sensing data could be used as a constraint for bottom-up emissions. In addition, we also found that daytime O_3 reductions over the outflow regions of LM following large reductions in NO_x emissions in the urban areas are significantly larger than they are over outflow regions of PC. These findings provide policymakers in the two regions with information critical to establishing strategies for mitigating air pollution.

1 Introduction

Nitrogen oxides ($NO_x = NO + NO_2$) are major O_3 precursors that originate from fossil fuel combustion, lightning, soil, aircraft, and biomass burning. The largest source of NO_x over North America is anthropogenic fossil fuel combustion (e.g., Hudman et al., 2007; Choi et al., 2009). Anthropogenic emissions significantly influence the variability of surface NO_x concentrations. Several previous studies have shown the proportionality of NO_x emissions to satellite-observed NO_2 column density (e.g., Berlie et al., 2003; Kim et al., 2006, 2009, 2011; Kaynak et al., 2009; Han et al., 2010; Yoshida et al., 2010; Lamsal et al., 2011; Choi et al., 2012). In particular, Berlie et al. (2003), Kaynak et al. (2009) and Choi et al. (2012) investigated the weekly cycles of the NO_x column density using retrieval products from Global Ozone Monitoring Experiments (GOME), SCanning Imaging Absorption spectroMeter for Atmospheric CartograpHY

ACPD
13, 21159–21201, 2013

(SCIAMACHY), or GOME2 and found the weekly pattern of the NO_2 column density proportional to that of NO_x emissions.

In general, atmospheric scientists obtain daily or weekly patterns of NO_x emissions through emissions inventory modeling (e.g., Sparse Matrix Operator Kernel Emissions (SMOKE) modeling, e.g., Houyoux et al., 2000) as in Choi et al. (2012). Although Community Multiscale Air Quality (CMAQ) model users have just begun to use the EPA National Emission Inventory of 2008 (NEI2008), it is still being distributed and tested. Therefore, the National Emission Inventory of 2005 (NEI2005) continues to be used in global and regional CTMs (e.g., the latest version of Weather Research and Forecasting-Chemistry, WRF-Chem) for the simulation of air quality and the impact of meteorological conditions on the chemical environment over the US. The NEI2005 was produced by a bottom-up approach from which a variety of anthropogenic and natural activities were taken into account, and the corresponding emissions efficiency for each activity was estimated (e.g., Hanna et al., 2003). Thus, as previous studies (e.g., Hanna et al., 2003; Napelenok et al., 2008; Kim et al., 2009, 2011; Han et al., 2010; Choi et al., 2012) have asserted that over some regions of the US, emissions inventory products from the bottom-up approach might exhibit uncertainty reaching a factor of two. Therefore, some other constraints may improve the evaluation/modification of the bottom-up emissions inventory.

Several previous studies pertaining to the NO_x emissions inventory of the EPA NEI have focused on investigating changes in the number of NO_2 columns resulting from either air pollution policy regulations over the eastern, western, and southern US (e.g., Kim et al., 2006, 2009, 2011; Choi et al., 2009, 2012; Russell et al., 2010) or over China (e.g., Zhao et al., 2009; Yang et al., 2011), or the occurrence of extreme weather conditions over coastal urban regions near the Gulf of Mexico (e.g., Yoshida et al., 2010). These studies have shown significant differences between the NO_2 column densities of two satellite instruments (OMI and SCIAMACHY) and WRF-Chem across the western United States (e.g., Kim et al., 2009). In particular, Kim et al. (2009) found that NO_x emissions from an updated NEI1998 in WRF-Chem in western urban areas such as

ACPD
13, 21159–21201, 2013

Los Angeles were overestimated, resulting in large discrepancies of the simulated NO_2 columns in the areas. Kim et al. (2011) also revealed differences between the NO_2 densities of OMI and those of WRF-Chem with NEI2005 in urban cities over Texas. Brioude et al. (2011) showed differences between the NO_y of the model and that of the National Oceanic and Atmospheric Administration (NOAA) and the National Center for Atmospheric Research (NCAR) research aircraft in and around Houston. They claimed that in the Houston Ship Channel (in the eastern part of Houston), either over-predicted NO_x emissions were another source of the discrepancies and speculated that surface O_3 over the region could be better simulated if there were fewer NO_x emissions.

Eder et al. (2009) showed large discrepancies (low or high) in the simulated surface O_3 concentrations from the real-time National Air Quality Forecast Capability (NAQFC) in urban areas of the southern California and Gulf Coast regions of the US. Several other studies focused on investigating causes for simulated surface O_3 biases in the urban areas (e.g., Eder et al., 2009; Zhang et al., 2007; Henderson et al., 2010; Kim et al., 2011). They showed that the uncertainty of the simulated PBL height (e.g., Eder et al., 2009), the emissions inventory of NO_x or VOC (e.g., Eder et al., 2009; Kim et al., 2009, 2011), meteorological uncertainties (e.g., Zhang et al., 2007), or model resolution (e.g., Henderson et al., 2010) introduce simulated O_3 biases. In particular, Kim et al. (2009, 2011) estimated the uncertainty of the emissions inventory by comparing the NO_2 column densities of the model and remote sensing, but they have not utilized remote-sensing data to derive or adjust the emissions inventory in the model. In some other studies, even with the large uncertainty in remote sensing data, atmospheric scientists have shown the feasibility of utilizing the satellite column density for yielding an accurate NO_x emissions inventory by using top-down satellite products for global CTMs (e.g., Martin et al., 2003; Lamsal et al., 2011) and regional CTMs (e.g., Choi et al., 2008; Napelenok et al., 2008; Chai et al., 2009; Zhao et al., 2009).

However, as addressed above, most of the previous studies have focused on the evaluation of the NO_x emissions inventory by comparing the NO_2 column of the model and remote sensing. Recently, Choi et al. (2012) showed that results from the CMAQ

ACPD
13, 21159–21201, 2013

model with satellite-adjusted NO_x emissions more accurately captured the weekly cycle of surface NO_x over the US for August 2009. In the study, they utilized the adjusted emissions inventory using remote sensing data and showed that a modified emissions inventory mitigates the discrepancies between the simulated weekly cycle of surface NO_x concentrations and the corresponding in-situ surface measurements. Thus, we concluded that understanding the impact of emissions changes on surface NO_x and O_3 concentrations is crucial to determining whether a top-down approach using remote-sensing data can be used for updating/constraining the bottom-up emissions inventory.

The main purpose of this study is not to obtain an accurate emissions inventory or estimate the absolute uncertainty of the emissions inventory, but instead to perform an evaluation of the relative uncertainties of both the NO_x emissions inventory and adjusted NO_x emissions inventories using remote sensing in the two urban areas that showed large discrepancies between simulated surface O_3 and corresponding observations. As we mentioned above, among these cities, Los Angeles and Houston have been investigated by previous NO_2 remote sensing studies (e.g., Kim et al., 2009, 2011; Eder et al., 2009) because of their characteristic as an O_3 nonattainment area and a large discrepancy area of simulated O_3 compared with in-situ measurements. Again, our previous study (Choi et al., 2012) showed how changes in NO_x emissions utilizing remote sensing products mitigate discrepancies between the weekly NO_x pattern at EPA AQS measurement stations produced by the model and that produced by observations. In this study, we use the same GOME-2-adjusted NO_x emissions inventory (details regarding on how the emissions inventory was obtained are described in Choi et al., 2012). With the simulation results from both baseline and sensitivity CMAQ with the adjusted emissions inventory for six geological regions – Pacific Coast = PC, Rocky Mountains = RM, Lower Middle = LM, Upper Middle = UM, Southeast = SE, and Northeast = NE) (Fig. 1) – we investigate (1) which geological region produces the largest NO_x differences between CMAQ and in-situ surface observations, (2) how satellite-adjusted emissions mitigate the simulated discrepancies of surface NO_x concentrations, (3) how the satellite-adjusted emissions affect surface O_3 discrepancies of

ACPD
13, 21159–21201, 2013

the model at the stations of two geological regions (PC and LM) of the urban cities, and (4) how changes in the emissions in the urban areas of the geological regions affect the surface O_3 over the outflow regions during the daytime.

2 Model and emissions

The CMAQ model, version 4.7.1 (Foley et al., 2010), was applied August 2009 over the CONUS domain using a horizontal resolution of 12 km with 22 vertical layers from the surface to 100 hPa. Meteorological data came from the NOAA National Centers for Environmental Prediction (NCEP) North American Model (NAM), which uses the Weather Research and Forecasting Non-hydrostatic Mesoscale Model (WRF-NMM) (e.g., Eder et al., 2009; Choi et al., 2012). This study used the SMOKE system to process all emissions independent from meteorological conditions (Houyoux et al., 2000) and generated emissions that vary with meteorological conditions in a pre-processor to CMAQ using NMM data fields (e.g., Eder et al., 2009; Choi et al., 2012). We based area and off-road engine emissions for the CMAQ simulations on NEI2005 version 1 and used the electric generating unit (EGU) and non-EGU sources as point sources in the US. Wherever it was possible in the inventory, we substituted continuous emissions monitoring (CEM) data in 2007 for EGU point sources and then updated and projected EGU emissions using emissions projection factors from the Department of Energy 2009 Annual Energy Outlook (AEO) to account for reductions in power plant emissions. Again, the number of point sources has decreased since 2005, and this reduction was determined using CEM data for 2007 and AEO 2009. For mobile sources, we used the EPA Office of Transportation and Air Quality (OTAQ) 2005 on-road emissions inventories and based the number of emissions from wildfires, prescribed burning, and residential wood burning on a multi-year average fire year of 1996–2002 (Choi et al., 2012). Estimations of biogenic VOC and NO emissions came from the Biogenic Emissions Inventory System (BEIS) version 3 (Houyoux et al., 2000). The baseline emissions and GOME-2-adjusted emissions over the US were 462 and 426 Gg N, re-

ACPD
13, 21159–21201, 2013

spectively, for August 2009. The baseline emissions (referred to as "BASE2009") were obtained from NEI2005, which accounted for reductions in the point sources addressed above. The GOME-2-adjusted emissions (referred to as "GOME2009") were obtained from BASE2009 and the GOME-2 and CMAQ NO_2 column ratios. Details relating to the chemistry modules and the chemical boundary conditions for this study were described in the previous study by Choi et al. (2012).

3 Measurements

3.1 The Global Ozone Monitoring Experiment-2 NO_2 column density

We used the remotely-sensed NO_2 column density from the Global Ozone Monitoring Experiment-2 (GOME-2) sensor to measure the nadir at 9.30 a.m. local time (LT) with footprints of $40 \times 80\,km^2$, obtained the daily GOME-2 NO_2 column retrievals from http://www.temis.nl/airpollution, and used TM4NO2A version 2.1 for the GOME-2 NO_2 column density. Details pertaining to the NO_2 column retrieval products and the reasons for using GOME-2 were provided in the study addressed by the previous studies (Choi et al., 2012 and other references in).

3.2 In-situ observed ground-level NO_x and O_3

Hourly ground-level NO_x and O_3 concentrations (measurement detection limit of 5 ppbv, J. Summers, personal communication from Choi et al., 2008) came from the EPA AQS website for 1100 (for O_3) and 265 (for NO_x) measurement stations in the CONUS domain for August 2009 (e.g., Choi et al., 2012). We mapped the measurement sites onto a 12 km CMAQ model domain, allowing for a total of 897 and 240 measurement-to-model comparison locations, and then used hourly NO_x and O_3 data to estimate model biases over the six geological regions. In addition, we chose four or five measurement-to-model comparison locations for the detailed study of the impact of changed emissions on surface NO_x and O_3 concentrations in the urban and outflow

ACPD
13, 21159–21201, 2013

areas of the two geological regions, PC and LM, and used the corresponding in-situ hourly NO_x and O_3 data to evaluate each comparison location.

4 Results

4.1 Comparison of the NO_2 columns of CMAQ to those of GOME-2

The monthly mean column retrievals for GOME-2 NO_2 retrievals and the equivalent column-integrated values of NO_2 concentrations were estimated for August 2009. Gorline and Lee (2010) showed that during the three-year period of 2007 to 2009, the month of August 2009 showed the greatest positive O_3 bias of the CMAQ-based National Air Quality Forecast Capability (NAQFC) modeling system. The other setup of CMAQ model showed several over- and under-estimates over CONUS during the summer in a previous study by Choi et al. (2012). The study also showed that a comparison of model-simulated and satellite-observed NO_2 columns exhibited general overestimates in concentrated population areas and underestimates in rural areas (e.g., Choi et al., 2012). In particular, the CMAQ model overestimated the NO_2 column over some urban areas of PC and LM (e.g., Los Angeles, CA, South Pasadena, CA, Anaheim, CA, La Habra, CA, Riverside, CA, Houston, TX, Beaumont, TX, and Sulphur, LA), also found by previous studies (e.g., Martin et al., 2006; Choi et al., 2008, 2009, 2012). The following subsections will discuss the impact of highly-biased NO_x emissions on surface NO_x and O_3 concentrations in the urban and outflow areas.

4.2 Satellite-adjusted NO_x emissions, GOME2009

To evaluate the NO_x emissions inventory of BASE2009 over six geological regions, we performed additional simulations with GOME2009 for August 2009. Again, this study focused on analyzing the relative uncertainty (instead of absolute uncertainty) of BASE2009 among the six geological regions. The sensitivity simulation, which determined the amount of NO_x emissions that increased or decreased according to the

ACPD
13, 21159–21201, 2013

ratio, found that NO_x emissions decreased by about 7.8 % over the US (from 462 Gg N to 426 Gg N), and changes in the amount of emissions varied in each geological region (e.g., PC = −5.6 %, RM = −12.3 %, LM = −21.3 %, UM = +2.3 %, SE = −15.9 %, NE = +10.0 %) (Table 1). The large reductions were shown in LM (17.5 Gg N) and SE (14.0 Gg N). The reductions may have been caused by reductions in mobile emissions because the consistent decrease in power plant NO_x emissions was accounted for in the baseline emissions, BASE2009, but because of the limited datasets for mobile emission reductions over the contiguous US, changes in mobile sources were not (e.g., Choi et al., 2012). Interestingly, the opposite trend showing an increase in NO_2 emissions appeared over NE (5.4 Gg N) in the satellite emissions, GOME2009. The trend showing an increase in GOME NO_2 columns over the geological region of NE from 1996 to 2002 was found in a previous study by Richter et al. (2005). Trends showing increased NO_x emissions over the region were not well simulated in the emissions modeling. Pickering et al. (2011) found some evidence of an increase in unresolved NO_x emissions sources in Pennsylvania, and other neighboring states. The explanation for these results remains unclear.

4.3 The impact of GOME2009 on surface NO_x over six geological regions

As we addressed above, the explanations for the large differences between the NO_2 columns of CMAQ and those of GOME-2 remain unclear. However, if we assume that GOME-2 involves an additional constraint on the emissions inventory, we could utilize the GOME-2 NO_2 columns to produce the GOME-2-adjusted emissions inventory, GOME2009. Then, by comparing model-simulated surface NO_x with in-situ surface observations, we could examine whether GOME2009 represents a useful constraint for a bottom-up emissions inventory. Initial comparisons of ground-level AQS NO_x observations in the six geological regions (black cross) to baseline CMAQ with the BASE2009 emissions (blue) and sensitive CMAQ (red) model simulations with the GOME2009 emissions are shown in Fig. 2. The figure displays a plot of observed (black crosses) and model-simulated (blue and red solid lines, representing baseline CMAQ

ACPD
13, 21159–21201, 2013

and CMAQ with GOME2009, respectively) NO_x concentrations at EPA AQS stations over the six geological regions in August 2009. The total number, mean, and standard deviations of AQS NO_x observations and corresponding CMAQ results are also estimated for all the measurement stations over six geological regions (Table 2). For AQS station measurements for PC, RM, LM, UM, SE, and NE regions with high correlation coefficients among hourly NO_x concentrations from observations and two CMAQ model runs ($0.70 < R < 0.84$), the biases of the baseline CMAQ with BASE2009 are both positive and negative (normalized mean bias, NMB = +19.8 %, −13.8 %, +149.7 %, +22.5 %, +31.3 %, +11.6 %); CMAQ simulations with GOME2009 improve in terms of the absolute amounts of NMB (NMB = −13.7 %, −36.7 %, −1.8 %, −7.8 %, −7.9 %, +0.7 %), except for the geological region, RM. Analysis of these six geological regions shows three noticeable changes in the biases: reductions in NMB from +149.7 % to −1.8 % over LM, from +31.3 % to −7.9 % over SE, and from +19.8 % to −13.7 % over PC. We also found that the biases of CMAQ with GOME2009, compared to those of corresponding AQS observations, were estimated as negative over five geological regions, possibly resulting from the contamination of NO_2 measurements resulting from the use of commercial chemiluminescence analyzers with molybdenum oxide converts at the measurement stations, described in previous studies (e.g., Lamsal et al., 2008 and other references in).

Particularly over LM and PC, the pronounced large reductions in simulated NO_x concentrations (in absolute amount) from the baseline to sensitivity CMAQ with GOME2009 (10.7 ppbv over LM and 4.7 ppbv over PC) (Table 2) suggest that NO_x emissions from BASE2009 at the EPA AQS stations of geological regions LM and PC are likely to be high. The reduction in simulated NO_x concentrations from the baseline CMAQ over SE was estimated to be 2.4 ppb at the EPA AQS stations, which is smaller than the reduction at the other stations over the LM and PC regions. The following sections will provide details regarding the impact of large reductions in NO_x emissions on surface NO_x and O_3 concentrations in the urban areas of the LM and PC regions. We developed the new emissions inventory, GOME2009, using the ratios of remote sens-

ACPD
13, 21159–21201, 2013

ing and the model and then evaluated the results from the CMAQ with GOME2009 by comparing them with the results of other in-situ surface observations in the urban areas and their outflow regions.

Considering all the uncertainties of the chemistry and transport in the model and remote sensing observations addressed by previous studies (e.g., Richter et al., 2005; Lamsal et al., 2008; Kim et al., 2011), the relatively high simulated NO_x biases from baseline CMAQ in urban areas over LM are likely the result of over-predictions of simulated NO_x emissions. Furthermore, the mean NO_x concentrations at AQS stations over PC from high NO_x emissions in urban areas such as Los Angeles are the largest (13.8 ppbv) (Table 2). Interestingly, whereas the baseline CMAQ over-predicted NO_2 columns compared to GOME-2 NO_2 columns in the urban areas in southern California, the model under-predicted NO_2 columns over neighboring rural regions. The explanations for the contrasting trends in the urban and rural areas are not clear, but by enhancing emissions in rural areas and reducing those values in urban areas, we can at least produce similar chemical environments in terms of the absolute amount of surface NO_x concentrations. By doing so, we can examine how changes in the chemical environments (by modifying NO_x emissions) impact surface NO_x and O_3 concentrations in the urban areas and their neighboring outflow regions of PC and LM.

4.4 The impact of GOME2009 on surface NO_x and O_3 concentrations over PC

As addressed in the previous section, the EPA AQS observations sites over PC yielded relatively higher NO_x concentrations than those of other geological regions (Table 2). In addition, the large discrepancies between simulated surface NO_x concentrations of baseline CMAQ simulation and those of AQS observations occurred in the urban areas of PC (Table 3), of which Los Angeles is a representative. To examine how large reductions in NO_x emissions in urban areas (e.g., 1: Los Angeles, 2: South Pasadena, 3: Anaheim, 4: La Habra, and 5: Riverside, CA) (Fig. 3) affect surface NO_x and O_3, we estimated the impact of large changes in emissions on surface concentrations in or near the urban cities during the daytime (LT, 01.00–05.00 p.m.) (Fig. 3). Large re-

ACPD
13, 21159–21201, 2013

ductions in emissions (> 3.0 mol s^{-1}) in the urban areas resulted in large reductions in surface NO_x concentrations in the cities (> 15.0 ppbv) (Fig. 3). In addition, several increases in NO_x emissions in the eastern parts of the urban cities in the satellite emission, GOME2009 (see the negative values on the left panel of Fig. 3) also appear, but the impact of changes in emissions on surface NO_x concentrations are not evident (see the right panel of Fig. 3), likely the result of the eastward transport of significantly reduced NO_x air in urban cities (Fig. 3). In conclusion, the large changes in surface NO_x emissions mitigated the large discrepancies in CMAQ simulated surface NO_x concentrations (see the circles on the right panel of Fig. 3), compared to corresponding EPA AQS observations (Fig. 3).

To evaluate how the GOME2009 emissions inventory affects the surface NO_x concentrations at five station grids (including the discrepancies of > 20 ppbv NO_x concentrations during the daytime (LT, 01.00–05.00 p.m.), compared to the corresponding EPA AQS observations), we estimate three sets of surface NO_x concentrations from CMAQ simulations with BASE2009, CMAQ simulations with GOME2009, EPA AQS observations (Table 3). Estimates of the mean values of the surface NO_x concentrations at the AQS sites were 34.7 ppbv, 24.7 ppbv, 20.3 ppbv, 21.5 ppbv, and 23.1 ppbv at the five station grids (1: Los Angeles, 2: South Pasadena, 3: Anaheim, 4: La Habra, and 5: Riverside) (Table 3). Estimated surface NO_x concentrations of the baseline CMAQ model were 59.6 ppbv, 52.2 ppbv, 43.4 ppbv, 38.5 ppbv, and 51.8 ppbv at the grids. The corresponding estimates from CMAQ with GOME2009 were 29.8 ppbv, 25.2 ppbv, 23.1 ppbv, 18.7 ppbv, and 31.2 ppbv, which were similar to those of EPA AQS observations.

Statistically, the baseline CMAQ model significantly over-predicted surface NO_x concentrations at the five station grids by +71.8 %, +111.3 %, +113.8 %, +79.1 %, and +124.2 % (Table 3). The high biases significantly decreased, becoming positive or negative values of −14.1 %, +2.0 %, +13.8 %, −13.0 %, and +35.1 % in the CMAQ simulation with GOME2009 emissions. The GOME2009 NO_x emissions significantly

ACPD
13, 21159–21201, 2013

mitigated the model-simulated discrepancies in surface NO_x concentrations at the five station grids (Fig. 4).

Because of the complexity of O_3 production, changes in surface O_3 following changes in NO_x emissions are more difficult to understand. Large reductions in NO_x emissions in urban cities such as Los Angeles result in large increases in daytime O_3 (LT, 01.00–05.00 p.m.) in the areas and the downwind from the urban cities is caused by westerly see breezes during the daytime in the summer. As Los Angeles is a typical NO_x-saturated regime area in the US, the large reductions in NO_x emissions resulted in large increases in surface O_3 concentrations in the urban city and its neighboring areas (see the right panel of Fig. 5). Interestingly, the CMAQ with BASE2009 emissions under-predicted surface O_3 in and near Los Angeles and South Pasadena and their outflow areas, including Riverside (up to 30 ppbv) (see the circles of the right panel of Fig. 5). Thus, the large increases in simulated surface O_3 following significant reductions in NO_x emissions in Los Angeles, Pasadena, and Anaheim resulted in trends of pre-existing simulated under-prediction to those of over-prediction in the areas (see the right panel of Fig. 5).

Large reductions in NO_x emissions resulted in reductions in NO_x concentrations and increases in O_3 concentrations in the urban cities (Figs. 4 and 5), which is a typical trend shown in NO_x-saturated regime areas. For example, the baseline CMAQ model under-predicted surface O_3 concentrations by −22.7 %, −27.1 %, −23.4 %, −13.1 % and −31.3 % at the five station grids, and the large reductions in NO_x emissions increased surface O_3 concentrations, which resulted in overestimation of the surface O_3 predictions of +37.6 %, +31.3 %, +19.5 %, +38.1 %, and +9.6 % (Table 4). In other words, the large reduction in NO_x emissions introduced the over-prediction of surface O_3 concentrations in CMAQ with GOME2009 (Fig. 6).

We also investigated how O_3 concentrations vary during the daytime (01.00–05.00 p.m., LT) from baseline CMAQ to CMAQ with the GOME2009 emissions. Similarly, during the daytime, the CMAQ model under-predicted surface O_3 concentrations by −12.9 %, −29.0 %, −24.8 %, −20.9 %, and −27.2 % at the five station grids,

ACPD
13, 21159–21201, 2013

and large reductions in NO_x emissions significantly increased surface O_3 concentrations; thus, the under-prediction patterns became over-prediction patterns of +25.4 %, +12.0 %, +11.5 %, +19.6 %, and +9.2 % at the five grids (see the parentheses in Table 4). During the daytime, except for the station in Los Angeles, the large biases of surface O_3 at the stations in South Pasadena, Anaheim, La Habra, and Riverside decreased as a result of reductions in NO_x emissions. The large NO_x reductions mitigated the large discrepancies between the NO_x concentrations of the baseline CMAQ and those of corresponding AQS observations and enhanced simulated surface O_3 concentrations, but the increases in O_3 concentrations were extreme, likely stemming from the high sensitivity of surface O_3 to changes in NO_x emissions. Interestingly, the low biases of baseline CMAQ during the daytime (01.00–05.00 p.m., LT) decreased in a more efficient manner than those of the baseline CMAQ during the whole day, even with the large increase in nighttime O_3 caused by a reduction in surface NO_x emissions (Fig. 6). Explanations for this phenomenon remain unclear, probably because the CMAQ model represents the urban areas as extreme NO_x-saturated regime areas (instead of normal NO_x-saturated areas or mixed areas, shown in Fig. 3 of the previous study by Choi et al., 2012), likely due to the overestimated NO_x emissions.

Several previous studies have also suggested that the uncertainty in the emissions of O_3 precursors such as NO_x is closely associated with large low O_3 biases over Southern California (e.g., Eder et al., 2009; Kim et al., 2009). Eder et al. (2009) related the changes in surface O_3 biases to incorrect temporal variations in NO_x emissions from the weekdays to the weekends. Kim et al. (2009) showed that two satellite (OMI and SCIAMACHY)-observed NO_2 columns are approximately twice as small as the corresponding WRF-Chem-simulated NO_2 columns in the urban areas along the US West Coast. They suggested that these differences were caused by overestimated NO_x emissions in the areas from an updated NEI1999 they used in their study. Again, in this study, unlike in previous studies, we reveal that with regard to satellite-adjusted emissions, GOME2009 mitigated simulated NO_x and daytime O_3 discrepancies compared to the corresponding observations.

ACPD
13, 21159–21201, 2013

4.5 The impact of GOME2009 on surface NO_x and O_3 concentrations over LM

Large discrepancies in the simulated surface NO_x concentrations were shown in the urban areas of LM compared to the corresponding in-situ observations (see the circles on the right panel of Fig. 7). To examine how the large reductions in NO_x emissions at the stations in the urban areas (e.g., Houston and Beaumont, TX and Sulphur, LA) (Fig. 7) affect surface NO_x and O_3, we investigated the impact of large changes in emissions on surface concentrations in or near the three urban cities over LM (Fig. 7). During the daytime (01.00–05.00 p.m., LT), the large reductions in emissions ($> 2.0\,mol\,s^{-1}$) in the urban areas resulted in reductions in surface NO_x concentrations in the cities (> 8.0 ppbv) (Fig. 7). In addition, some increases in NO_x emissions over the western parts of Houston resulted in increases in surface NO_x concentrations (> 2.0 ppbv) during the daytime (Fig. 7).

To investigate how satellite-adjusted emissions, GOME2009, affect surface NO_x concentrations in the model, we examine four station grids for the urban areas (Fig. 8). We chose the four grids because they exhibited large differences between the baseline CMAQ simulated and EPA AQS observed NO_x concentrations of > 10 ppbv during the daytime (01.00–05.00 p.m., LT) (see the right panel of Fig. 7). For more details, we compared the surface NO_x concentrations from baseline CMAQ and CMAQ with GOME2009 to the corresponding in-situ observations at the four different station grids (Fig. 8). Our analysis showed that the baseline CMAQ model over-predicted surface NO_x concentrations by +288.0 %, +464.2 %, +683.1 %, and +402.5 % at the four station grids (Table 5 and Fig. 8). Interestingly, from the baseline CMAQ, the diurnal differences in the surface NO_x concentrations in the urban areas of LM were significantly larger than those in the urban areas of PC. The baseline CMAQ significantly overestimated the surface NO_x, particularly during the nighttime in the urban areas of LM, partly because of the underestimated PBL heights over the Gulf Coast areas, as Eder et al. (2009) previously found.

ACPD
13, 21159–21201, 2013

The large reductions in NO_x emissions led to significant reductions in surface NO_x concentrations and thus mitigated the discrepancies between simulated surface NO_x concentrations of baseline CMAQ and the corresponding EPA AQS observations, and those of CMAQ with GOME2009 became as +15.8 %, +65.5 %, +172.7 %, and +46.8 % (Table 5 and Fig. 8). The CMAQ with GOME2009 still over-predicted surface NO_x concentrations at the four urban areas, but the overestimates of the baseline CMAQ model significantly decreased (Fig. 8).

The large reductions in NO_x emissions in the urban areas of the LM region generally resulted in large reductions in daytime O_3 (LT, 01.00–05.00 p.m.) over regions downwind from the urban cities (e.g., over forested regions represented by an extreme NO_x-sensitive regime) because of the distinctive southerly or southeasterly sea breezes during the daytime in the summer (see the right panel of Fig. 9). In another words, in the forested areas over the regions downwind from Houston and Beaumont, TX and Sulphur, LA (e.g., Sam Houston National Forest and Devy Crockell National Forest), monthly-averaged daytime O_3 concentrations significantly decreased by > 6 ppbv as a result of reductions in NO_x emissions in the urban cities (see the right panel of Fig. 9). During the summertime, dominant sea breezes from the ocean blow into the area following a large reduction in NO_x emissions in the central cities during the daytime, resulting in large O_3 reductions over the NO_x-sensitive regime regions (e.g., forested areas) (Fig. 9).

Large reductions in NO_x emissions resulted in several increases in surface O_3 concentrations in the core cities (e.g., Houston and Sulphur) (Table 6). For example, during the daytime (01.00–05.00 p.m., LT), the baseline CMAQ originally over-predicted surface O_3 (about 8 ppbv) in Houston and (about 2 ppb) Sulphur (see the parentheses of Table 6). Thus, the large increases in simulated surface O_3 following the significant reductions in NO_x emissions in central Houston and Sulphur exacerbated pre-existing simulated over-prediction trends in the areas (Table 6).

This study showed that overestimates of simulated surface O_3 in the urban centers or industrial areas were relatively smaller than those of the simulated surface O_3 in the

ACPD
13, 21159–21201, 2013

other areas of Houston (see the left panel of Fig. 9) likely the result of the limitation of the CMAQ model, that is, its inability to capture temporary high-peak O_3 phenomena in central or industrial areas. The monthly-averaged surface O_3 concentration plot does not fully represent specific-surface O_3 peaks near the Houston Ship Channel as Daum et al. (2003) and Xiao et al. (2010) showed in their studies. Thus, the ratio of VOC/NO_x as a proxy of the chemical environment needs further investigation.

We examined how the GOME2009 emissions impact surface O_3 concentrations at selected station grids, as we did in the NO_x study. At the four selected grids, the baseline CMAQ model revealed negative biases of simulated surface O_3 concentrations compared to corresponding observations (Fig. 10). At the four marked station grids, the baseline CMAQ model under-predicted surface O_3 concentrations by −7.2 %, −19.4 %, −36.6 %, and −18.6 % (see the blue colored line of Fig. 10). The large reductions in NO_x emissions (Fig. 7) generally increased surface O_3 concentrations and the under-prediction trends of CMAQ became weaker or changed to over-prediction trends. For example, at the four station grids, the estimates of the biases of the CMAQ model with GOME2009 emissions were +55.5 %, +18.5 %, −9.1 % and +38.1 % (see the red colored line of Fig. 10).

During the daytime (LT, 01.00–05.00 p.m.), estimates of the biases of the baseline CMAQ were +21.0 %, +17.9 %, −3.0 %, and +6.9 %, and emissions of the biases of the CMAQ with the GOME2009 changed to +39.1 %, +24.0 %, +3.2 %, and +20.7 % at the four station grids in the urban areas (see the parentheses of Table 6). The baseline CMAQ originally overestimated or slightly underestimated surface O_3 concentrations in the urban areas during the daytime, and the large reduction in the surface NO_x emissions resulted in the large increase in simulated surface O_3 concentrations in the areas. Thus, the increased surface O_3 concentrations from the model with GOME2009 increased trends of overestimation of the baseline CMAQ (Table 6).

Consistent with the results of a previous study by Choi et al. (2012), the results of this study show that CMAQ recognizes the central urban areas of LM as extreme NO_x-saturated regime areas (by the overestimates of NO_x emissions). The high-biased NO_x

ACPD
13, 21159–21201, 2013

concentrations in the urban cores might enhance surface O_3 more over the regions downwind from the urban cities (particularly in the forecasted areas in northeastern Houston) (Fig. 9). Because of the opposing chemical characteristics of these two areas regarding O_3 sensitivity (e.g., urban cores: NO_x-saturated area and forests: NO_x-sensitive area) to changes in NO_x emissions/concentrations, designing an efficient O_3 control strategy for both areas poses a challenge. Whereas Li et al. (2007) showed the impact of the reduction in biogenic VOC emissions in forested areas in northeastern Houston on surface O_3 in the urban core of Houston, this study showed the impact of the reduction in surface NO_x emissions in urban cores on surface O_3 over the outflow regions from Houston (Fig. 9).

The explanation for preexisting high O_3 biases (> 6 ppbv) in CMAQ in and around Houston (see the circles on the right panel of Fig. 9) remains unclear. However, the over-prediction of NO_x emissions in Houston, shown in Fig. 7, is likely a major cause of the over-predicted surface NO_x concentrations, and the large NO_x emissions reductions significantly mitigate the discrepancies of the baseline CMAQ compared to the corresponding AQS observations (see the right panel of Fig. 7), but the overestimated NO_x emissions cannot solely explain the over-prediction of the surface O_3 in the area. The large NO_x reductions in GOME2009 mitigated the high O_3 biases over the outflow region of and around the urban cities, but they exacerbated the O_3 high biases of the baseline CMAQ in the core of Houston and Sulphur (Table 6). In Beaumont, the large NO_x reductions increased the simulated surface O_3 concentrations, which resulted in mitigating low O_3 biases of the baseline CMAQ in urban areas such as Los Angeles.

From comparisons of WRF-Chem model results and aircraft and remote sensing measurements, Kim et al. (2011) concluded that the Houston NO_x emissions in NEI2005 were overestimated and the Houston VOC emissions in NEI2005 were underestimated. They hypothesized that less NO_x and more VOC emissions in the Houston industrial area might have introduced better O_3 modeling performance, but they still found large deficiencies in model-simulated O_3 even when they accounted for these two factors and suggested the need for future study that would clarify the O_3 high bias

ACPD
13, 21159–21201, 2013

issue. The results of this study showed that significant reductions in NO_x emissions (more than those found by Kim et al., 2011) mitigate the discrepancies of the simulated NO_x concentrations both in the urban and outflow areas from the baseline CMAQ, but they do not mitigate the discrepancies of the simulated O_3 concentrations in the urban core areas. The results from this study also showed that the large reductions in NO_x emissions in urban cities lead to large reductions in simulated surface O_3 over the outflow regions around the urban cities, which would be critical for mitigating the simulated O_3 discrepancies over the outflow regions.

5 Conclusion and discussion

To evaluate the baseline emissions inventory, BASE2009, we analyzed simulation results from CMAQ over six geological regions over the CONUS. We adjusted the NO_x emissions inventory, GOME2009, from BASE2009 over the CONUS using ratios of CMAQ to GOME-2 NO_2 column density. We found large reductions in NO_x concentrations in CMAQ with the satellite-adjusted emissions, GOME2009, at EPA AQS stations over LM, SE and PC (i.e., +149.7 % to −1.8 % for LM, +31.3 % to −7.9 % for SE, and +19.8 % to −13.7 % for PC), which resulted from large reductions in NO_x emissions over the regions. The GOME2009 significantly reduced the biases of the surface NO_x concentrations in the urban areas of the LM and PC regions of CMAQ simulations and EPA AQS observations, resulting in the mitigation of the simulated discrepancies of the baseline CMAQ.

The results of this study indicated that NO_x emissions from BASE2009 in the urban areas of the LM (e.g., Houston, Beaumont, and Sulphur) and PC regions (e.g., Los Angeles, South Pasadena, Anaheim, La Habra, and Riverside) are abnormally high, indicating large relative uncertainty of BASE2009 NO_x emissions in the urban areas. The analysis of simulation results from global/regional CTMs and climate models must account for these high NO_x biases in the urban areas of LM and PC. For example, significant reductions in NO_x emissions led to large reductions in model simulations of

ACPD
13, 21159–21201, 2013

surface NO_x at EPA AQS stations in the urban areas of LM and PC. In particular, in the urban areas of the LM region, the largest discrepancies in simulated surface NO_x concentrations are significantly mitigated in the areas, compared to the corresponding NO_x observations from EPA AQS. These results suggest that the remote sensing-derived GOME2009 emissions inventory could be another useful constraint of the bottom-up emissions inventory. Furthermore, changes in NO_x emissions in the urban areas of LM and PC in GOME2009 compared to those in BASE2009 are useful for not only updating the emissions inventory but also mitigating the discrepancies in the chemical environment such as those in NO_x concentrations.

In general, while the large reductions in NO_x emissions in GOME2009 mitigated the discrepancies in the simulated O_3 concentrations in the urban areas of the PC region (e.g., South Pasadena, La Habra and Riverside) and the LM region (e.g., Beaumont), the large reductions in emissions exacerbated the over-predictions of pre-existing high-biased surface O_3 in urban core areas (particularly in Houston and Sulphur) of the LM region in the baseline CMAQ simulations resulting from the increase in surface O_3 from reductions in NO_x emissions. However, the large reductions in NO_x emissions mitigate the high O_3 biases over the outflow region or around the main core of Houston (see the right panel of Fig. 9). Again, reductions in the over-predictions of pre-existing simulated large O_3 in the urban core cities of the LM regions in the baseline CMAQ did not occur as a result of reductions in the high over-predictions of NO_x emissions except in Beaumont; thus, to explain simulated high O_3 bias over the southern US from CTMs, shown in previous studies (e.g., McKeen et al., 2009; Kim et al., 2011), we need to divide urban areas into urban core cities and near or outflow regions of the urban core areas and test the two regions separately. In addition to NO_x concentrations, the emissions of VOCs over the LM and PC regions require further investigation. In future research, we will introduce another remote sensing product such as HCHO columns as a proxy for VOC measurements. In addition, we will divide high O_3-biased regions into chemical regime regions, which might prove useful for determining the cause of high O_3 biases.

ACPD
13, 21159–21201, 2013

As Kim et al. (2011) stated, if we have more VOC emissions and fewer NO_x emissions in the industrial areas of Houston, we might simulate similar chemical environments in the areas in terms of the ratios of VOC/NO_x. However, they also showed that simulated O_3 concentrations still exhibit large discrepancies compared to in-situ observed O_3 concentrations. In a future study, we will first modify the chemical environment (both NO_x and VOC) in the areas, which might alter the chemical characteristics of an extreme NO_x-saturated regime region to those of a less NO_x-saturated regime region or a mixed regime region in industrial and urban areas. For example, as we addressed above, as a proxy for VOC emissions, we will also evaluate simulated HCHO column densities in the model and compare them to remote sensing HCHO column densities. After performing this evaluation, we can evaluate the ratio of the simulated HCHO/NO_2 column densities (as a proxy for the chemical environment, VOC/NO_x) to those of corresponding remote-sensing observations. Of course, one challenge of this task is how we consider the uncertainty of remote sensing, such as that stemming from the products of HCHO columns.

This study also found that during the summertime, the significant reduction of NO_x emissions in urban core cities resulted in an increase in surface O_3 concentrations in the urban areas (e.g., Los Angeles, South Pasadena, Anaheim, La Habra, Riverside, Houston, Beaumont, and Sulphur), but resulted in large reductions in surface O_3 concentrations in forested areas or outflow regions over northeastern or northern regions downwind from urban cities (e.g., Houston and Beaumont). These large reductions are not clearly shown in the outflow regions of urban cities in southern California (e.g., near Los Angeles) likely because of lower VOC concentrations in the outflow regions. In other words, while the NO_x-saturated regime regions become NO_x-sensitive regime regions as the location moves from the urban cities of Houston and Beaumont of the LM region to their outflow rural or forested regions, the characteristics of the NO_x-saturated regime of the urban area of Los Angeles remain stable, as do those of the outflow region from the urban city because of limited VOC sources. In a future study, we plan to investigate how quickly the chemical regime from urban areas to outflow

ACPD
13, 21159–21201, 2013

areas changes in the United States, the purpose of which is to design an optimal O_3 pollution control strategy for each urban area.

The direct satellite-adjusting method in this study gave general success in mitigating the discrepancies of model-simulated surface NO_x concentrations compared with in-situ measurements, but further research is needed to addresses some of remaining issues. First, the assumption that remote-sensing NO_2 columns are closer to actual true values compared with model-simulated NO_2 columns was not perfectly met by the results. Thus, ideally, in order to get accurate emission inventories, we need to estimate uncertainties of remote-sensing NO_2 column and model simulated NO_2 column/NO_x emission inventories and use the uncertainties for the application of data assimilation approach (e.g., Napelenok et al., 2008; Chai et al., 2009; Zhao et al., 2009). Second, emissions were adjusted using morning time satellite NO_2 column data (e.g., GOME-2) and the resulting emission inventory could miss its diurnal cycle. In a following study, we will adjust the diurnal cycles of emissions using two different remote sensing data from GOME-2 (morning time) and OMI (afternoon). Some other uncertainties regarding the use of NO_2 columns as a proxy for NO_x concentrations/emissions over the surface were described in detail in the previous study (Choi et al., 2012).

Acknowledgements. This work is dedicated to the memory of Dr. Daewon Byun (1956–2011), whose pursuit of scientific excellence as a developer of the CMAQ model continues to inspire us. I thank Daniel Tong and Hyuncheol Kim for the preparation of the emissions data, Pius Lee and other NOAA ARL and NWS group members, and Barry Lefer, Robert Talbot, Xun Jiang, and atmospheric science graduate students at the University of Houston for their useful comments. I also acknowledge the free use of tropospheric NO_2 column data from the GOME-2 sensor from www.temis.nl.

References

Beirle, S., Platt, U., Wenig, M., and Wagner, T.: Weekly cycle of NO_2 by GOME measurements: a signature of anthropogenic sources, Atmos. Chem. Phys., 3, 2225–2232, doi:10.5194/acp-3-2225-2003, 2003.

ACPD
13, 21159–21201, 2013

Brioude, J., Kim, S.-W., Angevine, W. M., Frost, G. J., Lee, S.-H., McKeen, S. A., Trainer, M., Fehsenfeld, F. C., Holloway, J. S., Ryerson, T. B., Williams, E. J., Petron, G., and Fast, J. D.: Top-down estimate of anthropogenic emission inventories and their interannual variability in Houston using a mesoscale inverse modeling technique, J. Geophys. Res., 116, D20305, doi:10.1029/2011JD016215, 2011.

Chai, T., Carmichael, G. R., Tang, Y., Sandu, A., Heckel, A., Richter, A., and Burrows, J. P.: Regional NO_x emission inversion through a four-dimensional variational approach using SCIAMACHY tropospheric NO_2 column observations, Atmos. Environ., 43, 5046–5055, 2009.

Choi, Y., Wang, Y., Zeng, T., Cunnold, D., Yang, E., Martin, R., Chance, K., Thouret, V., and Edgerton, E.: Spring to summer northward migration of high O_3 over the western North Atlantic, Geophys. Res. Lett, 35, L04818, doi:10.1029/2007GL032276, 2008.

Choi, Y., Kim, J., Eldering, A., Osterman, G., Yung, Y. L., Gu, Y., and Liou, K. N.: Lightning and anthropogenic NO_x sources over the United States and the western North Atlantic Ocean: impact on OLR and radiative effects, Geophys. Res. Lett, 36, L17806, doi:10.1029/2009GL039381, 2009.

Choi, Y., Kim, H., Tong, D., and Lee, P.: Summertime weekly cycles of observed and modeled NO_x and O_3 concentrations as a function of satellite-derived ozone production sensitivity and land use types over the Continental United States, Atmos. Chem. Phys., 12, 6291–6307, doi:10.5194/acp-12-6291-2012, 2012.

Daum, P. H., Kleinman, L. I., Springston, S. R., Nunnermacker, L. J., Lee, Y.-N., Weinstein-Lloyd, J., Zheng, J., and Berkowtiz, C. M.: A comparative study of O_3 formation in the Houston urban and industrial plumes during the 2000 Texas Air Quality Study, J. Geophys. Res., 108, 4715, doi:10.1029/2003JD003552, 2003.

Eder, B., Kang, D., Mathur, R., Pleim, J., Yu, S., Otte, T., and Pouliot, G.: A performance evaluation of the National Air Quality Forecast Capability for the summer of 2007, Atmos. Environ., 43, 2312–2320, 2009.

Foley, K. M., Roselle, S. J., Appel, K. W., Bhave, P. V., Pleim, J. E., Otte, T. L., Mathur, R., Sarwar, G., Young, J. O., Gilliam, R. C., Nolte, C. G., Kelly, J. T., Gilliland, A. B., and Bash, J. O.: Incremental testing of the Community Multiscale Air Quality (CMAQ) modeling system version 4.7, Geosci. Model Dev., 3, 205–226, doi:10.5194/gmd-3-205-2010, 2010.

Gorline, J. and Lee, P.: Performance of NOAA-EPA Air Quality Prediction, 2007–2009 CMAS conference 2010, available at: www.cmascenter.org/conference/2009/abstracts/gorline_performance_noaa-epa_2009.pdf (last access: 9 August 2013), 2010.

ACPD
13, 21159–21201, 2013

Han, K. M., Lee, C. K., Lee. J., Kim, J., and Song, C. H.: A comparison study between model-predicted and OMI-retrieved tropospheric NO_2 columns over the Korean peninsula, Atmos. Environ., 45, 2962–2971, 2010.
Hanna, S. R., Lu, Z., Frey, H. C., Wheeler, N., Vukovich, J., Arunachalam, S., Fernau, M., and Hansen, D. A.: Uncertainties in predicted ozone concentrations due to input uncertainties for the UAM-V photochemical grid model applied to the July 1995 OTAG domain, Atmos. Environ., 35, 891–903, 2003.
Henderson, B. H., Jeffries, H. E., Kim, B. U., and Vizuete, W. G.: The influence of model resolution on ozone in industrial volatile organic compound plumes, J. Air Waste Manage., 60, 1105–1117, 2010.
Houyoux, M. R., Vukovich, J. M., Coats, C. J., Wheeler, N. J.M, Kasibhatla, P. S.: Emission inventory development and processing for the Seasonal Model for Regional Air Quality (SMRAQ) project, J. Geophys. Res., 105, 9079–9090, 2000.
Hudman, R. C., Jacob, D. J., Turquety, S., Leibensperger, E. M., Murray, L. T., Wu, S., Gilliland, A. B., Avery, M., Bertram, T. H., Brune, W., Cohen, R. C., Dibb, J. E., Flocke, F. M., Fried, A., Holloway, J., Neuman, J. A., Orville, R., Perring, A., Ren, X., Sachse, G. W., Singh, H. B., Swanson, A., and Wooldridge, P. J.: Surface and lightning sources of nitrogen oxides over the United States: magnitudes, chemical evolution, and outflow, J. Geophys. Res., 112, D12S05, doi:10.1029/2006JD007912, 2007.
Kaynak, B., Hu, Y., Martin, R. V., Sioris, C. E., and Russell, A. G.: Comparison of weekly cycle of NO_2 satellite retrievals and NO_x emission inventories for the continental US, J. Geophys. Res., 114, D05302, doi:10.1029/2008JD010714, 2009.
Kim, S. W., Heckel, A., McKeen, S. A., Frost, G. J., Hsie, E.-Y., Trainer, M. K., Richter, A., Burrows, J. P., Peckham, S. E., and Grell, G. A.: Satellite observed US power plant NO_x emission reductions and their impact on air quality, Geophys. Res. Lett., 33, 122812, doi:10.1029/2006GL027749, 2006.
Kim, S. W., Heckel, A., Frost, G. J., Richter, A., Gleason, J., Burrows, J. P., McKeen, S., Hsie, E.-Y., Granier, C., and Trainer, M.: NO_2 columns in the western United States observed from space and simulated by a regional chemistry model and their implications for NO_x emissions, J. Geophys. Res., 114, D11301, doi:10.1029/2008JD011343, 2009.
Kim, S.-W., McKeen, S. A., Frost, G. J., Lee, S.-H., Trainer, M., Richter, A., Angevine, W. M., Atlas, E., Bianco, L., Boersma, K. F., Brioude, J., Burrows, J. P., de Gouw, J., Fried, A., Gleason, J., Hilboll, A., Mellqvist, J., Peischl, J., Richter, D., Rivera, C., Ryerson, T., te Lin-

ACPD
13, 21159–21201, 2013

tel Hekkert, S., Walega, J., Warneke, C., Weibring, P., and Williams, E.: Evaluations of NO_x and highly reactive VOC emission inventories in Texas and their implications for ozone plume simulations during the Texas Air Quality Study 2006, Atmos. Chem. Phys., 11, 11361–11386, doi:10.5194/acp-11-11361-2011, 2011.

Lamsal, L. N., Martin, R. V., van Donkelaar, A., Steinbacher, M., Celarier, E. A., Bucsela, E., Dunlea, E. J., and Pinto, J. P.: Ground-level nitrogen dioxide concentrations inferred from the satellite-borne Ozone Monitoring Instrument, J. Geophys. Res., 113, D16308, doi:10.1029/2007JD009235, 2008.

Lamsal, L. N., Martin, R. V., Padmanabhan, A., van Donkelaar, A., Zhang, Q., Sioris, C. E., Chance, K., Kurosu, T. P., and Newchurch, M. J.: Application of satellite observations for timely updates to global anthropogenic NO_x emission inventories, Geophys. Res. Lett., 38, L05810, doi:10.1029/2010GL046476, 2011.

Li, G., Zhang, R., Fan, J., and Tie, X.: Impacts of biogenic emissions on photochemical ozone production in Houston, Texas, J. Geophys. Res., 112, D10309, doi:10.1029/2006JD007924, 2007.

Martin, R. V., Jacob, D. J., Chance, K., Kurosu, T. P., Palmer, P. I., and Evans, M. J.: Global inventory of nitrogen oxide emissions constrained by space-based observations of NO_2 columns, J. Geophys. Res., 108, 4537, doi:10.1029/2003JD003453, 2003.

Martin, R. V., Sioris, C. E., Chance, K., Ryerson, T. B., Bertram, T. H., Wooldridge, P. J., Cohen, R. C., Neuman, J. A., Swanson, A., and Flocke, F. M.: Evaluation of space-based constraints on global nitrogen oxide emissions with regional aircraft measurements over and downwind of eastern North America, J. Geophys. Res., 111, D15308, doi:10.1029/2005JD006680, 2006.

McKeen, S., Grell, G., Peckham, S., Wilczak, J., and Djalaova, I.: An evaluation of real-time air quality forecasts and their urban emissions over eastern Texas during the summer of 2006 Second Texas Air Quality Study field study, J. Geophys. Res., 114, D00F11, doi:10.1029/2008JD011697, 2009.

Napelenok, S. L., Pinder, R. W., Gilliland, A. B., and Martin, R. V.: A method for evaluating spatially-resolved NO_x emissions using Kalman filter inversion, direct sensitivities, and space-based NO_2 observations, Atmos. Chem. Phys., 8, 5603–5614, doi:10.5194/acp-8-5603-2008, 2008.

ACPD
13, 21159–21201, 2013

Pickering, K., Prados, A., and Napelenok, S.: Monitoring Air Quality Changes in Regions Influenced by Major Point Sources over the Eastern and Central United States Using Aura/OMI NO_2, 2011 CMAS conference, 2011.

Richter, A., Burrows, J. P., Nub, H., Granier, C., and Niemeier, U.: Increase in tropospheric nitrogen dioxide over China observed from space, Nature, 437, 129–132, 2005.

Russell, A. R., Valin, L. C., Bucsela, E. J., Wenig, M. O., and Cohen, R. C.: Space-based constraints on spatial and temporal patterns of NO_x emissions in California, 2005–2008, Environ. Sci. Technol., 44, 3608–3615, 2010.

Xiao, X., Cohen, D. S., Byun, D. W., and Ngan, F.: Highly nonlinear ozone formation in the Houston region and implications for emission controls, Environ. Sci. Technol., 115, D23309, doi:10.1029/2010JD014435, 2010.

Yang, Q., Wang, Y., Zhao, C., Liu, Z., Gustafson, W. I., and Shao, M.: NO_x emission reduction and its effects on ozone during the 2008 Olympic Games, Environ. Sci. Technol., 45, 6404–64210, 2011.

Yoshida, Y., Duncan, B. N., Retscher, C., Pickering, K. E., Celarier, E. A., Joiner, J., Boersma, K. F., and Weefkind, J. P.: The impact of the 2005 Gulf Hurricanes on pollution emissions as inferred from Ozone Monitoring Instrument (OMI) nitrogen dioxide, Atmos. Environ., 44, 1443–1448, 2010.

Zhang, F., Bei, N., Nielsen-Gammon, J. W., Li, G., Zhang, R., Stuart, A., and Aksoy, A.: Impacts of meteorological uncertainties on ozone pollution predictability estimated through meteorological and photochemical ensemble forecasts, J. Geophys. Res., 112, D04304, doi:10.1029/2006JD007429, 2007.

Zhao, C. and Wang, Y.: Assimilated inversion of NO_x emissions over East Asia using OMI NO_2 column measurements, Geophys. Res. Lett., 36, L06805, doi:10.1029/2008GL037123, 2009.

ACPD
13, 21159–21201, 2013

Table 1. NO_x emissions inventory changes from baseline emissions inventory for August of 2009 (BASE2009) and GOME-2-adjusted emission inventory (GOME2009) over six geological regions of the US (PC: Pacific Coast, RM: Rocky Mountain, LM: Lower Middle, UM: Upper Middle, SE: Southeast, and NE: Northeast) for August 2009 (in unit of Gg N). The parentheses indicate the changes in the amounts of emissions in each geological region (in %).

Six geological regions	BASE2009	GOME2009	Difference
PC	48.9	46.2	−2.7 (−5.6 %)
RM	78.5	68.8	−9.6 (−12.3 %)
LM	82.2	64.7	−17.5 (−21.3 %)
UM	110.8	113.4	+2.6 (+2.3 %)
SE	88.0	74.0	−14.0 (−15.9 %)
NE	53.8	59.2	+5.4 (+10.0 %)
Total	462.2	426.3	−35.9 (−7.8 %)

ACPD
13, 21159–21201, 2013

Table 2. The total number, the mean, and the standard deviation of the EPA AQS NO_x observations (in ppbv), CMAQ NO_x simulations with the base emissions, BASE2009 and CMAQ NO_x simulations with the GOME-2 adjusted emissions, GOME2009 at the EPA AQS NO_x measurement sites over six geological regions of the US (PC: Pacific Coast, RM: Rocky Mountain, LM: Lower Middle, UM: Upper Middle, SE: Southeast, and NE: Northeast).

		CMAQ with BASE2009 (NO_x)		CMAQ with GOME2009 (NO_x)		EPA AQS (NO_x)	
	N	mean	σ	mean	σ	mean	σ
PC	57 069	16.6	6.4	11.9	5.2	13.8	8.5
RM	18 479	6.5	3.0	4.8	2.4	7.6	3.8
LM	32 633	17.6	9.7	6.9	4.0	7.1	3.4
UM	13 442	13.9	7.4	10.4	5.7	11.3	7.3
SE	13 560	7.9	3.8	5.5	2.7	6.0	3.8
NE	27 130	12.3	4.8	11.1	4.4	11.0	5.1

ACPD
13, 21159–21201, 2013

Table 3. The total number, the mean, and the standard deviation of the EPA AQS NO_x observations (in ppbv), CMAQ NO_x simulations with the baseline emissions, BASE2009 and CMAQ NO_x simulations with GOME-2 adjusted emissions, GOME2009 at the five EPA AQS NO_x measurement sites (see the right panel of Fig. 3, 1: Los Angeles, 2: South Pasadena, 3: Anaheim, 4: La Habra, and 5: Riverside).

		CMAQ with BASE2009 (NO_x)		CMAQ with GOME2009 (NO_x)		EPA AQS (NO_x)	
	N	mean	σ	mean	σ	mean	σ
1	703	59.6	29.4	29.8	16.0	34.7	33.6
2	713	52.2	22.3	25.2	12.0	24.7	16.9
3	713	43.4	20.8	23.1	12.2	20.3	23.4
4	706	38.5	18.8	18.7	10.5	21.5	17.8
5	706	51.8	26.6	31.2	19.5	23.1	28.6

ACPD
13, 21159–21201, 2013

Table 4. The total number, the mean, and the standard deviation of the EPA AQS O_3 observations (in ppbv), CMAQ O_3 simulations with the baseline emissions, BASE2009 and CMAQ O_3 simulations with GOME-2 adjusted emissions, GOME2009 at the five EPA AQS O_3 measurement sites (see the right panel of Fig. 3, 1: Los Angeles, 2: South Pasadena, 3: Anaheim, 4: La Habra, and 5: Riverside). The parentheses indicate the corresponding data during the daytime (01.00–05.00 p.m., LT).

		CMAQ with BASE2009 (O_3)		CMAQ2 with GOME2009 (O_3)		AQS (O_3)	
	N	mean	σ	mean	σ	Mean	σ
1	700 (155)	21.8 (45.3)	20.6 (18.2)	38.8 (65.2)	25.8 (21.4)	28.2 (52.0)	23.1 (19.4)
2	713 (155)	24.0 (44.8)	20.8 (19.2)	43.2 (70.7)	26.4 (23.5)	32.9 (63.1)	28.0 (23.6)
3	713 (155)	25.2 (38.0)	18.6 (17.6)	39.3 (56.3)	21.2 (19.5)	32.9 (50.5)	18.3 (13.6)
4	706 (155)	27.8 (43.1)	19.9 (17.2)	44.2 (65.2)	24.2 (22.2)	32.0 (54.5)	21.3 (15.8)
5	706 (155)	25.7 (53.9)	27.7 (23.7)	41.0 (80.8)	33.3 (24.9)	37.4 (74.0)	29.2 (16.1)

ACPD
13, 21159–21201, 2013

Table 5. The number, the mean, and the standard deviation of the EPA AQS NO_x observations (in ppbv), CMAQ NO_x simulations with the baseline emissions, BASE2009 and CMAQ NO_x simulations with GOME-2 adjusted emissions, GOME2009 at the four different EPA AQS measurement sites (see the right panel of Fig. 7, 1: Houston A, 2: Houston B, 3: Beaumont, and 4: Sulphur).

		CMAQ with BASE2009 (NO_x)		CMAQ with GOME2009 (NO_x)		EPA AQS (NO_x)	
	N	mean	σ	mean	σ	mean	σ
1	727	61.3	51.2	18.3	21.6	15.8	13.5
2	732	83.5	70.4	24.5	24.7	14.8	11.2
3	615	60.3	39.4	21.0	14.3	7.7	6.0
4	643	39.7	22.8	11.6	6.6	7.9	4.1

ACPD
13, 21159–21201, 2013

Table 6. The number, the mean, and the standard deviation of the EPA AQS O_3 observations, CMAQ O_3 simulations with the baseline emissions, BASE2009 and CMAQ O_3 simulations with GOME-2 adjusted emissions, GOME2009 at the four EPA AQS O_3 measurement sites (see the right panel of Fig. 7, 1: Houston A, 2: Houston B, 3: Beaumont, and 4: Sulphur). The parentheses indicate the corresponding data during the daytime (01.00–05.00 p.m., LT).

		CMAQ with BASE2009 (O_3)		CMAQ with GOME2009 (O_3)		EPA AQS (O_3)	
	N	mean	σ	Mean	σ	mean	σ
1	738 (155)	19.4 (46.1)	20.1 (16.1)	32.3 (53.0)	18.4 (11.7)	20.9 (38.1)	17.1 (18.4)
2	740 (155)	18.3 (48.7)	22.4 (16.3)	26.9 (51.2)	20.8 (10.6)	22.7 (41.3)	18.1 (19.2)
3	737 (154)	16.1 (38.9)	20.1 (16.8)	23.1 (41.4)	17.2 (10.3)	25.4 (40.1)	18.3 (17.9)
4	730 (155)	15.8 (35.6)	18.1 (16.3)	26.8 (40.2)	13.7 (10.4)	19.4 (33.3)	15.2 (13.2)

ACPD
13, 21159–21201, 2013

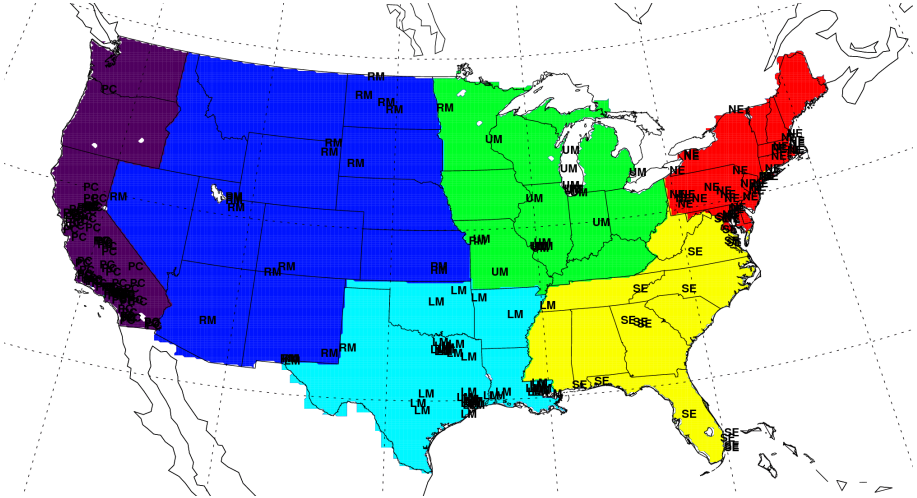

Fig. 1. Map of the six geological regions of the US, Pacific Coast (PC), Rocky Mountains (RM), Lower Middle (LM), Upper Middle (UM), South East (SE), and Northeast (NE) for the performance evaluation (different colors represent six geological regions and letters locate EPA AQS stations of NO_x measurements).

ACPD
13, 21159–21201, 2013

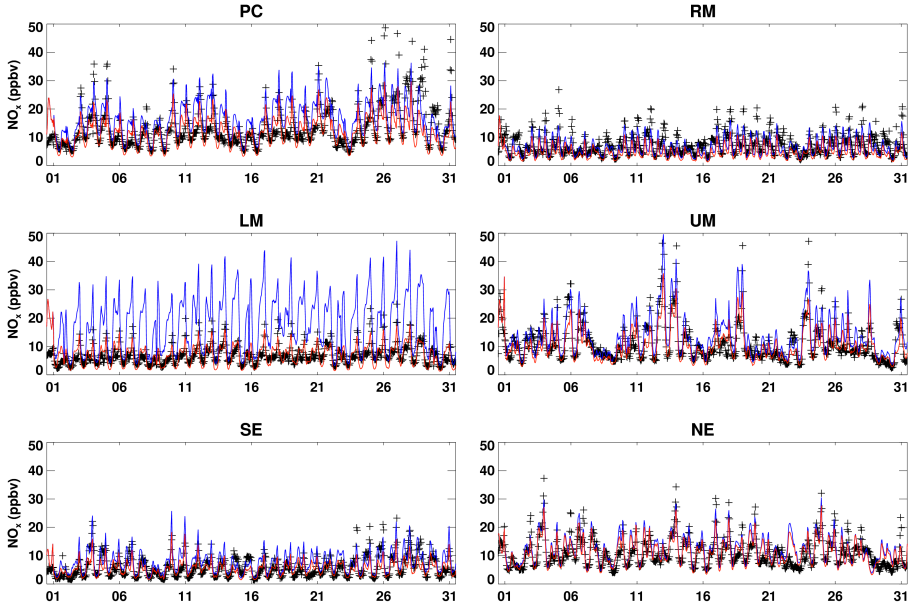

Fig. 2. Surface NO_x concentrations at EPA AQS stations (black crosses), corresponding CMAQ simulations with the baseline emissions, BASE2009 (blue), and CMAQ simulations including GOME-2-adjusted NO_x emissions, GOME2009 (red) over six geological regions (see Fig. 1, PC: Pacific Coast, RM: Rocky Mountain, LM: Low Middle, UM: Upper Middle, SE: South East, and NE: North East) for August 2009.

ACPD
13, 21159–21201, 2013

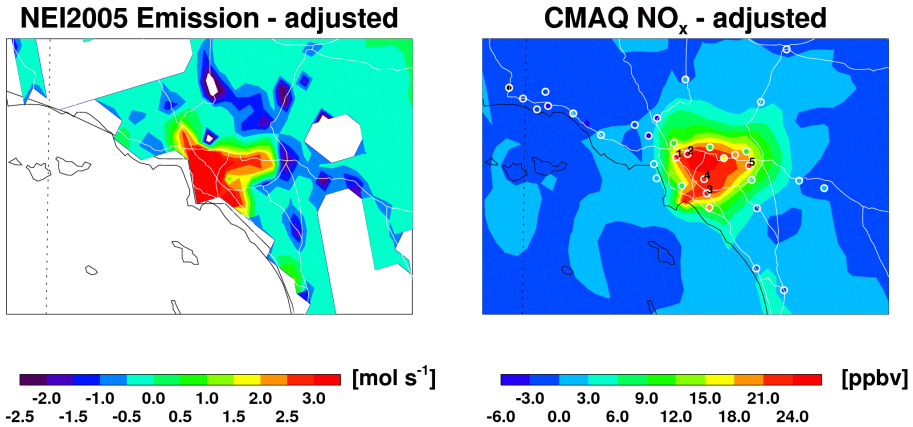

Fig. 3. The difference between the surface NO_x emissions of the baseline emissions BASE2009 and GOME-2-adjusted emissions GOME2009 (left panel, the difference is estimated only when monthly NO_2 column averages are $> 10^{15}$ molecules cm^{-2} from GOME-2 and CMAQ over the continent); the differences between the surface NO_x concentrations of the baseline CMAQ with BASE2009 and CMAQ with GOME2009 (right panel); and the differences between the baseline CMAQ with BASE2009 and EPA AQS observations (circles on the right panel) for the daytime (LT, 01.00–05.00 p.m.) of August 2009. Among the circled stations, the five marked stations (1: Los Angeles, 2: South Pasadena, 3: Anaheim, 4: La Habra, and 5: Riverside) include large discrepancies in > daytime 20 ppbv NO_x (baseline CMAQ simulations - EPA AQS observations).

ACPD
13, 21159–21201, 2013

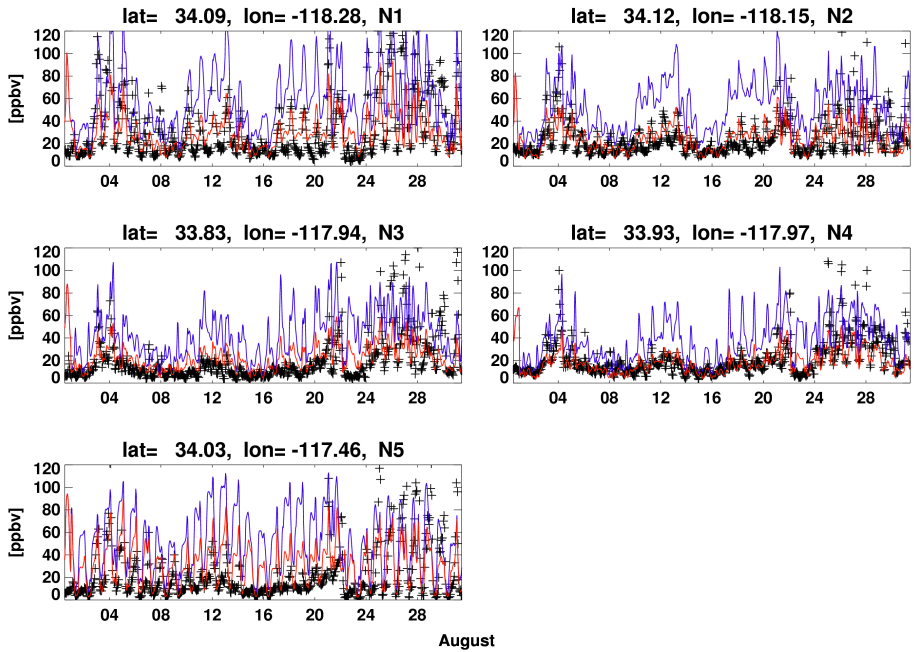

Fig. 4. Surface NO_x concentrations at EPA AQS stations (black crosses), corresponding baseline CMAQ simulations with baseline emissions, BASE2009 (blue), and CMAQ simulations with GOME-2-adjusted NO_x emissions, GOME2009 (red) at the five station grids (see the right panel of Fig. 3, 1: Los Angeles, 2: South Pasadena, 3: Anaheim, 4: La Habra, and 5: Riverside) in August 2009.

ACPD
13, 21159–21201, 2013

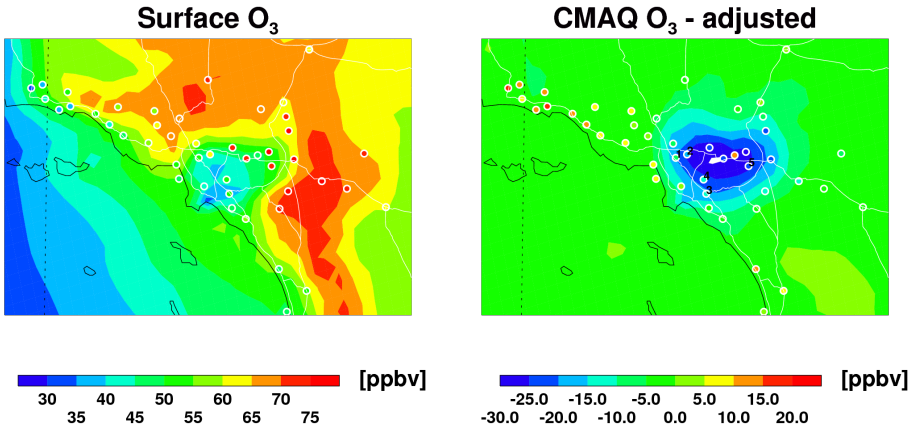

Fig. 5. Surface O_3 concentrations from the baseline CMAQ with baseline emissions, BASE2009 (left panel), and EPA AQS measurements (circles on the left panel), the difference between the surface O_3 of the baseline CMAQ with BASE2009 and CMAQ with GOME-2-adjusted NO_x emissions GOME2009 (right panel) and the difference between the surface O_3 of the baseline CMAQ with BASE2009 and EPA AQS (circles on the right panel, baseline CMAQ simulations - EPA AQS observations) for the daytime (LT, 01.00–05.00 p.m.) in August 2009.

ACPD
13, 21159–21201, 2013

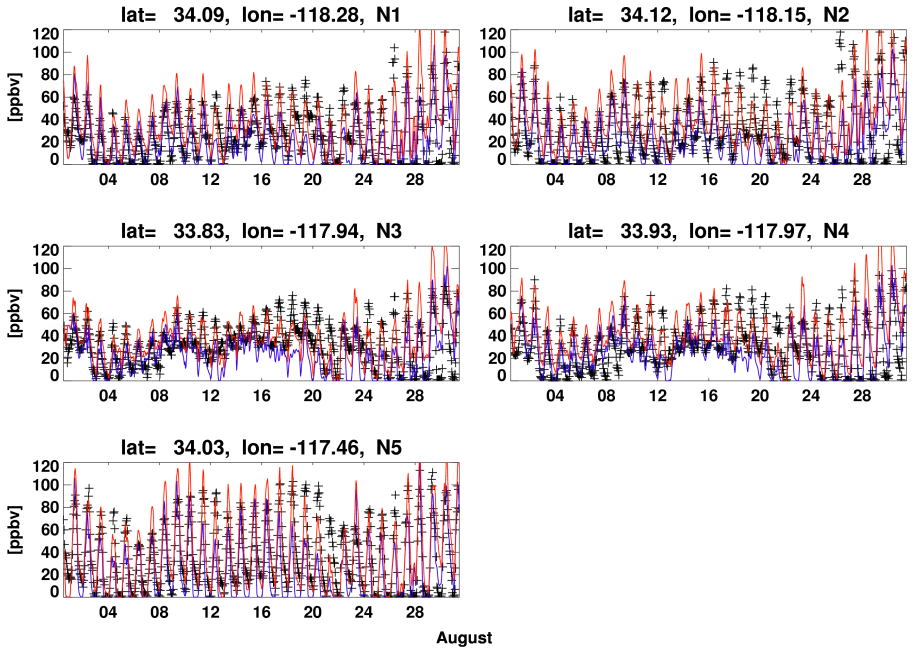

Fig. 6. Surface O_3 concentrations at EPA AQS stations (black crosses), corresponding baseline CMAQ simulations with baseline emissions, BASE2009 (blue), and CMAQ simulations with GOME-2-adjusted NO_x emissions, GOME2009 (red) at the five station grids (see the right panel of Fig. 3, 1: Los Angeles, 2: South Pasadena, 3: Anaheim, 4: La Habra, and 5: Riverside) in August 2009.

ACPD
13, 21159–21201, 2013

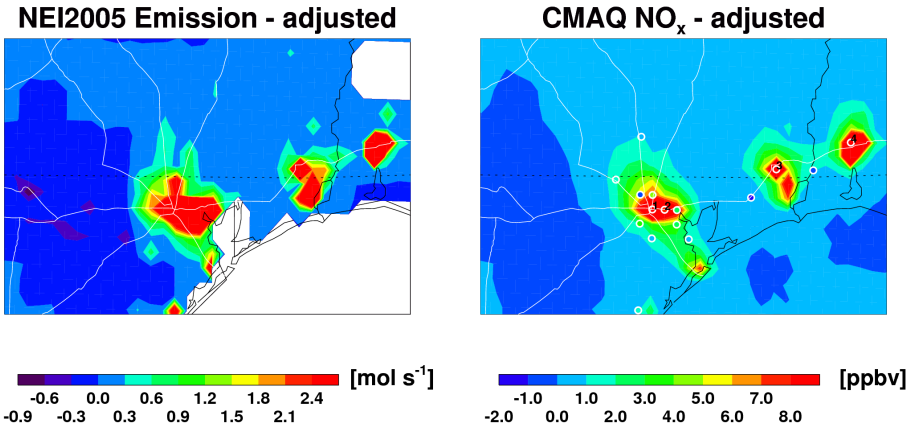

Fig. 7. The differences between surface NO_x emissions of baseline emissions, BASE2009 and GOME-2-adjusted emissions, GOME2009 (left panel, the difference is estimated only when monthly NO_2 column averages are $> 10^{15}$ molecules cm^{-2} from GOME-2 and CMAQ over the continent); the differences between the surface NO_x concentrations of the baseline CMAQ with BASE2009 and CMAQ with GOME2009 (right panel); and the differences between surface NO_x concentrations of the baseline CMAQ with BASE2009 and EPA AQS observations (circles on the right panel) for the daytime (LT, 01.00–05.00 p.m.) of August of 2009. Among the circled stations, the four marked stations (1: Houston A, 2: Houston B, 3: Beaumont, and 4: Sulphur) include the large discrepancies of > daytime 10 ppbv NO_x (baseline CMAQ simulations – EPA AQS observations).

ACPD
13, 21159–21201, 2013

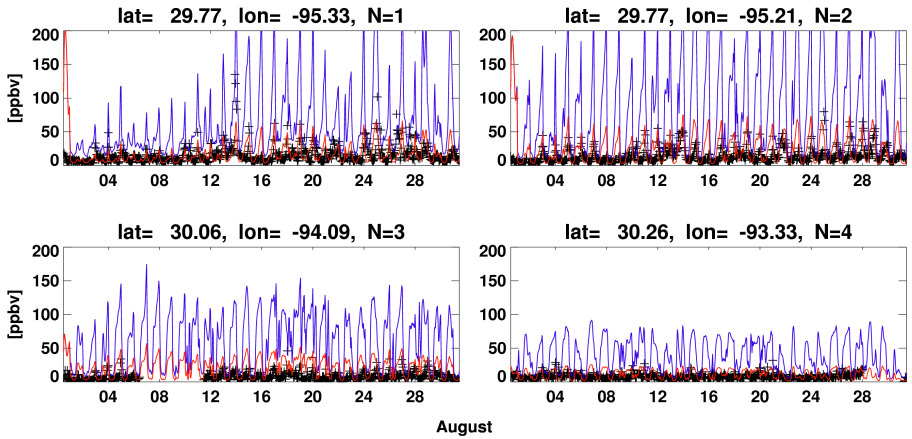

Fig. 8. Surface NO_x concentrations at EPA AQS stations (black crosses), corresponding baseline CMAQ simulations with baseline emissions, BASE2009 (blue), and CMAQ simulations with GOME-2-adjusted NO_x emissions, GOME2009 (red) at the four station grids (see the right panel of Fig. 7, 1: Houston A, 2: Houston B, 3: Beaumont, and 4: Sulphur) in August 2009.

ACPD
13, 21159–21201, 2013

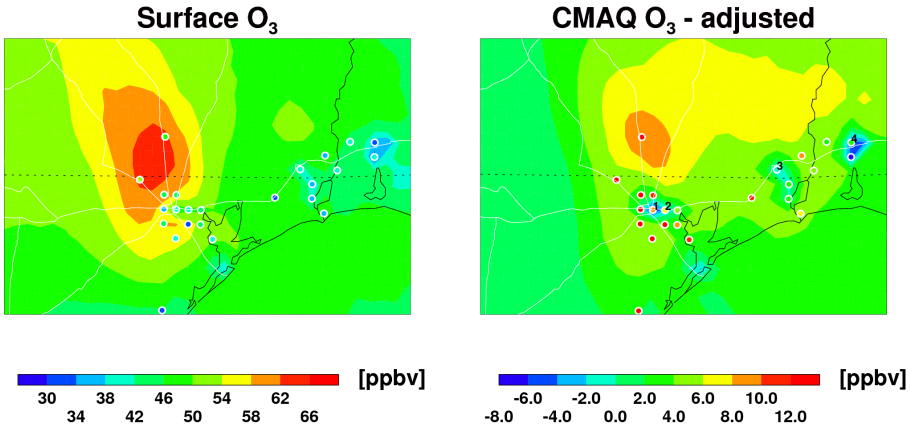

Fig. 9. The differences between the O_3 concentrations from a baseline CMAQ with baseline emissions, BASE2009 (left panel) and EPA AQS measurements (circles on the left panel); the differences between surface O_3 of the baseline CMAQ with BASE2009 and CMAQ with GOME-2-adjusted NO_x emissions, GOME2009 (right panel); and the differences between surface O_3 of the baseline CMAQ with BASE2009 and EPA AQS (circles on the right panel, baseline CMAQ simulations – EPA AQS observations) for the daytime (01.00–05.00 p.m., LT) of August of 2009.

ACPD
13, 21159–21201, 2013

Satellite-adjusted NO_x emissions on simulated NO_x and O_3 discrepancies

Y. Choi

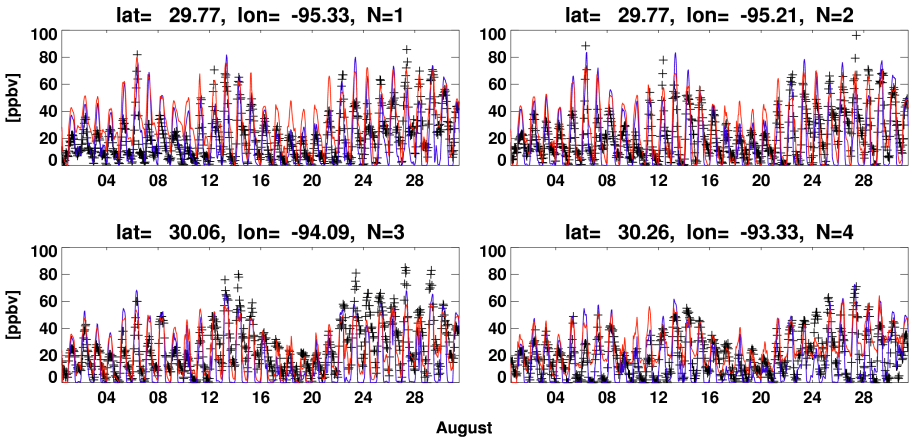

Fig. 10. Surface O_3 concentrations at EPA AQS stations (black crosses), corresponding baseline CMAQ simulations with baseline emissions, BASE2009 (blue), and CMAQ simulations with GOME-2-adjusted NO_x emissions, GOME2009 (red) at the four station grids (see the right panel of Fig. 7, 1: Houston A, 2: Houston B, 3: Beaumont, and 4: Sulphur) in August 2009.

ACPD
13, 21159–21201, 2013